Tautomated Colorectal Lymphoma Volume Calculation Using 3d Mri Images

Manu M R, Dr. B Balamurugan
India

Abstract: The third most prevalent cause of cancer death in the world is colorectal lymphoma (CL). Future disease burden predictions advise health planners and raise awareness about the need for action on cancer control. The lymphoma volume is usually estimated by means of magnetic resonance imaging (MRI), which analyses mutation during medical diagnosis at advanced stages. The precise segmentation of abnormal tissue and its correct 3D display is key to appropriate treatment. Here, there is an intention to build a smart diagnostic system based on the human MRI research. The suggested model presenting identification, Segmentation and 3D visualization method, offering medical specialists' expertise an efficient way for the 3D reconstruction of colorectal lymphoma using medical image processing in two-dimensional magnetic resonance images. Here the rectal MR images are Preprocessed that can be done using the weighted adaptive median filtering and uplift laplacian partial differential equation for further enhancement. Followed by preprocessing the Iterative Multi-linear component analysis was used for extracting the features. The extracted features can be given as an input for the CNN based Multiscale phase level set segmentation process. In this suggested segmentation, the abnormal resection margin is automatically analyzed and shows that this is consistent with traditional segmentation algorithm. Finally, a 3D simulation of the lymphoma of the colon is accomplished using the logical frustum model used for medical data rendering. The feasibility of the method suggested is confirmed by the 98.7% accuracy of the Colon MRI dataset. A subjective comparative analysis between the proposed approach and other state of art methods is also carried out as out in the work mentioned. The findings of experiments show a higher performance of the system than conventional systems, which support radiologists in measuring lymphoma size, structure and position in the colon.
Keywords: Colorectal Lymphoma, MRI, Lymphoma volume, weighted adaptive median filtering, uplift laplacian partial differential equation, Iterative Multi-linear component analysis, CNN based Multiscale phase level set segmentation, 3D reconstruction modeling, logical frustum model.

1. INTRODUCTION

Gastrointestinal systems (GI) or digestive systems are components of colon and rectum. The colon is associated with the rectum and begins from the small gut, also known as the big intestine. The key function is the consumption and disposal of salts, nutrients and water. New cancer figures have now diagnosed colorectal cancer as the second leading cause of cancer mortality in the United States. MRI is today the recommended form of diagnostic imaging for colorectal cancer primary diagnosis for the preparation of radiological treatment. Use of volumetric MRI data to delineate colorectal lymphoma areas manually by an oncologist or a radiologist. This time consuming and complicated manual delimitation or segmentation is variable between and within the observer. Since this saves time and minimizes human interference, successful automatic colorectal lymphoma segmentation methods in clinical radiation are also required for segmenting massive volumetric data into the colorectal lymphoma.Medical images are also messier because of the slice types of cancer regions. Compared with the images. Therefore, automatically segmenting colorectal lymphoma is a very difficult process, not only because of its limited scale but because the distribution of its shape and severity is not consistent. The auto section of colorectal volumetric 3D RMI has proven to be decent in recent years. Deep learning and machine-based learning approaches recently were widely used with excellent results in medical image segmentation
:The thesis of 3D volumetric segmentation provides a new means of solving the above problems. The proposed 3D Logical Frustum Model to expand the recently launched 2D segmentation of the volume network. To sum up, the degree of the multiscale the segmentation for colorectal lymphoma segmentation was employed with the following: (1) When low and high-scale features are generated regardless of each scale, a 3D Multiscale phase level set segmentationtraining device that has dense connections is used. An Iterative Multi-linear component analysisis used throughout the network to improve segmentation efficiency effectively. (2) The proposed network is based on learning and volume interfering which eliminates computational consistency. (3) A method that is superior to earlier baseline approaches is checked for the segmentations of the colorectal lymphoma in 3D MR images. The proposed approach can be used for more medical imaging applications depending on the incentives obtained with MR images. The paper can be organized accordingly: Section 1 presents a brief overview of and predictive problems with the colorectal lymphoma infrastructure. Section 2 reports a literature review of techniques to reduce the problem of

_____

prediction of colorectal lymphoma. Section 3 showed the problem argument. Section 4 tackled the problem of predictions defeating processes. The findings of the proposed procedure are then presented in Section 5 and the hypotheses are discussed

2. LITERATURE SURVEY

Some of the existing framework involved in the same Colorectal lymphomawork and others which include,
[1]We suggest that HL-FCN, a volumetrically entirely convolutionary network architecture effectively trained with hybrid loss, is automatically segmented in colorectal cancer regions. A new hybrid dice based loss is built on a Multi-Task Learning System to solve the issue of class imbalances and thus increase the capacity for discrimination. A technical ensemble multi-resolution model often reduces false positives, while maintaining limit detail. [2] Suggest a cascade learning strategy that reduces the consequences of these artefacts. It consists of (a) a number of new invariant features that cover valuable detailed information about presence and area type; and (b) a new level of formulation that moves the evolution of the contour around the probabilistic appearance of the region theoretically. [3] consider a whole different framework for the segmentation from bottom to bottom of colorectal polyps. This method would create a map of the same size as the original image of the input network . [4] Creation and assessment of recent progress in the measurement of ambiguities and models in the light of colonoscopy images semantic polyp segmentation. [5] Use of H and E stained tissue samples to calculate the effect of colorectal cancer in a deeper study classification and only the prognostic discrimination resulting from epithelial compartment of the CNN characteristics was compared with the visually-defined histological level. [6] Perform accurately predicting the probability of each picture produced by the network by incorporating several models To test the proposed method, the ETIS-LariPolypDB database has been used, and the conclusions show that our proposed method produces the state-of-the-art outcomes.[7] DoubleU-Net is suggested and at the same time defines initials and diagnoses histological groups and incorporate text diagnosis data so that the final segmentation is more accurate . [8] proposed an ensemble approach to performance improvement by integrating the two R-CNN Mask models with different backbone architectures (ResNet50 and ResNet101). [9] Presents a post-processing automated module to fine-tune deep network segmentation. The LAGAN group strengthens the generative adversarial (GAN) network by the labelling of profound network outputs. [10] Present a new artificial colorectal cancer segmentation approach built on the Convolutionary Neural Network (CNN). The algorithm used consists of several steps: a pre-processing step to normalise and light up the area of the tumour; a CNN classification step; and a post-processing step for reducing false positive effects. [11] Searched for an optimal segmentation strategy which satisfies the preliminary criteria: Identify major liver arteries, be sustainable and have little customer input . [12] proposed the use of imaging methods to segment colorectal lymphoma. [13] Proposed Computer Aided Diagnostic (CAD) System for reducing dependence on doctors experience and diagnostic capacity, and for timely and precise identification of previous tissue lesions. [14] For segmenting and classifying epithelial and stromal regions in histopathological photographs, a deep involutionary neural network was proposed. [15] propose a novel way to use a context-aware neural network built on images with a resolution of 17921792 pixels to include a larger context. The framework suggested encodes a local historological image into high-dimensional features, then adds the features to establish a final forecast in accordance with their spatial arrangement.

S.no	Title	Reference	Algorithm	Advantage	Disadvantage
1.	HL-FCN: Hybrid loss guided FCN for colorectal cancer segmentation	[1]	volume-to-volume fully convolution network	Less computation time	Less detection accuracy
2.	A cascade-learning approach for automated segmentation of tumour epithelium in colorectal cancer	[2]	cascade-learning approach	High detection accuracy	Training errors are high

3	Colorectal polyp segmentation using a fully convolutional neural network	[3]	fully convolutional neural network	Less training time	Layers confusion
4	Uncertainty and interpretability in convolutional neural networks for semantic segmentation of colorectal polyps	[4]	CNN	Less training and testing error	Large training data needed
5	Deep learning for tissue microarray image-based outcome prediction in patients with colorectal cancer	[5]	CNN	Less training and testing error	Donot encode the position
6	Colorectal Segmentation Using Multiple Encoder-Decoder Network in Colonoscopy Images	[6]	encoder-decoder network	High range of the detecting probability	Unexplained behavior of the network
7	DoubleU-Net: Colorectal Cancer Diagnosis and Gland Instance Segmentation with Text-Guided Feature Control	[7]	DoubleU-Net	Less training time	High error over image analysis problem
8	Ensemble of instance segmentation models for polyp segmentation in colonoscopy images	[8]	Mask R-CNN	Less training time	Lack of ability to be spatially invariant to the input data.
9	Accurate colorectal tumor segmentation for CT scans based on the label assignment generative adversarial network	[9]	generative adversarial network	High detection accuracy	Hard to train
10	A Convolutional Neural Network based system for Colorectal cancer segmentation on MRI images	[10]	new Convolutional Neural Network	Less training time	Generation of result is complex
11	Segmentation of hepatic vessels from MRI images for planning of electroporation-based treatments in the liver	[11]	Optimal segmentation	High detection accuracy	Increase segmentation cost
12	Colorectal Cancer MRI Image Segmentation Using Image Processing Techniques	[12]	K-means	Very fast	Hard to train
13	Automatic Colorectal Segmentation with Convolutional Neural Network	[13]	CNN	Less training time	Cannot handle numerical data
14	A Deep Convolutional Neural Network for segmenting and classifying epithelial and stromal regions in histopathological images	[14]	DCNN	Computationally faster	Difficult to predict variable
15	Context-Aware Convolutional Neural Network for Grading of Colorectal Cancer Histology Images	[15]	context-aware neural network	Easy to implement	High cost
16	Automated Classification and Segmentation in Colorectal Images Based on Self-Paced Transfer Network	[16]	Self paced transfer network	Easy to train	complexity and inability to recover from database corruption.

_____

Here several methods are discussed each of them having some disadvantages. Hence there is a need of an efficient system to overcome research gaps over existing methodologies.

3. PROBLEM STATEMNET

Existing research shows that the quality of the lesion segmentation results more efficiently. The current methods often use shape that ignores characteristics such as homogeneity. Similarly, there are procedures for detecting abnormalities in Colon MRI images that consider the small number of features. These procedures do not achieve validation effectiveness and precision. In addition, the various features to be used for segmentation are not considered in this technique. The lower segmentation precision and greater time complexity impair colorectal detection performance.

4. PROPOSED METHODOLOGY

The suggested framework is summarized in Figure1. This framework shows an improvement in comparison with previous attempts. This describes the components of a procedure that can be used to view the colorectal lymphoma in a 3D way. This describes colon MRI segmentation information, source and algorithms and 3D reconstruction from the colorectal obtained image data. On the Cancer Imaging Archive, the proposed method is largely validated.
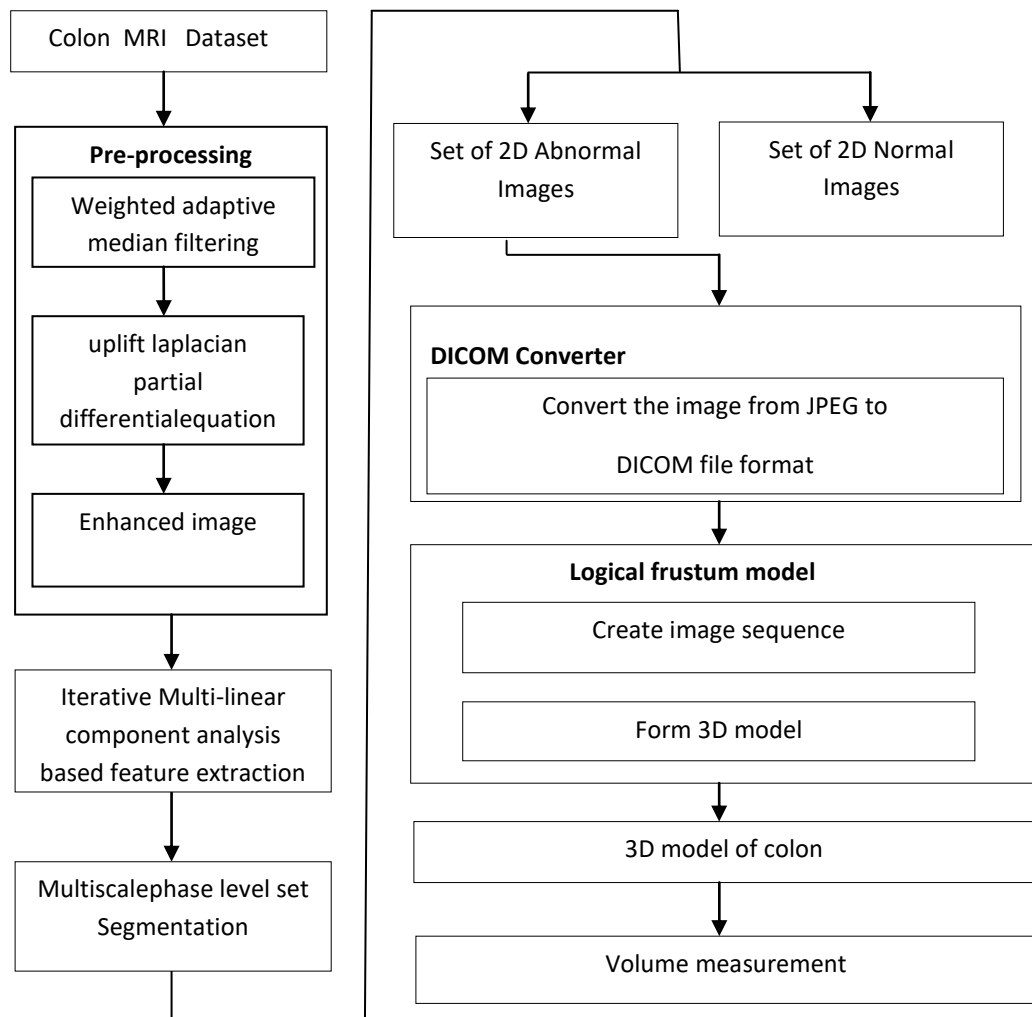

Figure 1   Schematic representation of the suggested methodology

a. Preprocessing

Magnetic Resonance Image (MRI) was used for the colon lymphoma images. The preprocessing phase was done before the process of feature extraction and image segmentation. The filtering process is used in the preprocessing step. The weighed adaptive Median Filter (WAMF) implements for the noise reduction in grey level images, fine picture information, lack of data substituted and difference in intensity by decreasing the quantity, thus modifying the neighboring pixels. The reduction of noise in MRI images is an effective method. Median filter is tested here for noise reduction. A weighed adaptive median filter is a simple technique used to eliminate noise from MR images. The median is determined by ordering the pixel approval and then the pixel consideration is moved to the Centre of the pixel ranking. The filter calculates the difference between the pixels by replacing each pixel by the average of adjacent pixels. Within original MR images, the filter can be used to determine the noise without sharpness reduction conditions. Consider the feedback of the noise-consistent image v (a, b). First, the image must be divided into L-level numbers, each level having one pixel value middle. Now, delete the noise by using the WAMF value estimates to replace the middle pixel. The equation of the weighed adaptive median filter is given

$$S(a, b) = \text{median}_{(s, t) \epsilon} C_{xy} \{k (u, v)\} \qquad (1)$$

Where, C_{xy} is the set of rectangular sub-image levels, centered at the point (x, y). This process is repeated for the entire level present in the input image when the speckle noise to be removed. Finally, to obtain the noise-free image in the preprocessing stage. However, the irregular signals may be suggested to improve the partial differential equation-based laplacian model. Thus, the algorithm is reformulated as a partial equation of variance.

$$, \partial P(l, m, n)/\partial t = f(l,m,n) - P^* (l,m,n) \quad (2)$$

In (1) $P(l, m, n)$ represents the continuous signal while f(i,j,k) = f {P(l,m,n)} = FINT {P (l,m,n)} and by implementing the finite difference method, the following expression can be obtained,

$$P^{t+1}(i,j) = P^t(i,j) + [\{P(l,m,n) - P^* (l,m,n)\}]\Delta t \qquad (3)$$

The enhancement of the image was done in this step. Therefore, the modified expression can be obtained by applying the anisotropic diffusion form,

$$\emptyset P(l, m, n)/ \emptyset t = \mu c_{RN}(\|\nabla P (l, m, n)\|) \text{ div } (\nabla P(l, m, n)/ \|\nabla P (l, m, n)\|) + f(l,m,n) - P (l,m,n) \qquad (4)$$

Where μ is a weighing factor that maintains the process of smoothing, $\nabla P (l, m, n)$ is the gradient of the signal, c_{RN} is the diffusion co-efficient.

$$c_{RN} = \|\nabla P (l, m, n)\| = 1/1 + [\|\nabla P (l, m, n)\|/k]^2 \quad (5)$$

The word μ affects the degree to which the equation is lightened with a higher smoothing value. Signals can, however, be reinforced before smoothing. But the signal is sharpened and masked with the signal by linear signal amplification operators such as Laplacian. Therefore there is a need to sharpen the source input selectively and balance out the surroundings in order to avoid noise rise. The explosive volatility and still want to prevent Reverse method of heat diffusion. The method of forward and backward diffusion can be applied according to laplacian as,

$$c_{FBD}(\|\nabla P (l, m, n)\| = 1/1 + [\|\nabla P (l, m, n)\|/f_k]^n - \alpha/1 + \|\nabla S (i, j, k^2 * P)\| - f_k)\vartheta]^2m \qquad (6)$$

The method is unsuitable for the protection of texture and is appropriate for image signal fluidification. Therefore, the smoothing needs to proceed with a rational rate of sharpening without modifying the signal. Hence, the equation was changed with the Laplacian introducing the updated expression:

$$\emptyset P(l, m, n)/\emptyset t = \mu \; c_{FBD}(\|\nabla P (l, m, n)\| \text{ div } \frac{\nabla P (l, m, n)}{\|\nabla P (l, m, n)\|} + [f(l,m,n) - P (l,m,n)] - \mu\Delta^2 P(i,j,k)$$

(7)

This results in the generalized PDE-based smoothing/sharpening formulation and the improved initial continuous image field S(l,m,n) as,

$$\emptyset P(i. j, k)/\emptyset t = \mu \; g_{FBD} \; ([P(l, m, n)) + g_e (P(l, m, n) + \mu g_e (S(l, m, n) \qquad (8)$$

Where $g_{FBD} (P(l, m, n))$, $g_e (P(l, m, n)$, $\mu g_e (P(l, m, n)$ represents the simultaneous sharpening functions that be expressed as,

_____

$$g_{FBD}\ (P(l, m, n)\ =\ c_{FBD}\ (\|\nabla P\ (l, m, n)\|)\ \text{div}\ (\frac{\nabla P\ (l,m,n)}{\|\nabla P\ (l,m,n)\|}\ )$$

(9)

The enhancement form of the PDE can be represented as,

$$g_{FBD}\ (P(l, m, n) = f(g_{FBD}\ (P(i. j)\ -\ (P(l, m, n))$$　　　　　(10)

The sharpening function can be represented as,

$$g_{FBD}(P(l, m, n){=}\Delta^2\ P(l, m, n)$$　　　　(11)

The above expression can sharpen the input signal.

b. Feature extraction

The texture parameters are extracted using the Iterative multi-linear component analysis (IMCA) are computed to study the identification of the colon lymphoma in the MRI image. This paper introduces linear discriminant regression for the collection of functions. The IMCA can be segregated as the unregulated learning since it generates the most autonomous part vectors. The input distribution of this approach, is connected to the classification problem. Consider the two Q1 and Q2 features which are distributed uniformly on [-1, 1] binary and the O output class and which are given below,

$$J{=}\begin{cases}0\ if\ Q1 + Q2\ < 0 \\ 1\ if\ Q1 + Q2\ \geq 0\end{cases}(12)$$

In this dilemma are the data points provided in the shady regions. The problem is linear separable and the required features of Q1 + Q2 can easily be chosen. The IMCA uses N-dimensional vectours, showing the route for the function space, in the set of data provisioners. This vector provides the best knowledge of the problem and the new feature that throws the output class into space (Q1, Q2). The matrix between the class S_{qr} is extracted for each and every class and S_{qs} are described as S_{qs} within the class Sqr,

$$P_{qs} = \sum_{a=1}^{pQ} P_a\ ; P_a = \frac{1}{p_s}\sum_{q \in q_s}(p - m_a)(q - m_a)^T (13)$$

$$P_{kr}{=} \sum_{a=1}^{kr}(m_a - m)(m_a - m)^T (4)$$

The d x d is the A matrix used and reduce dimensionality to render d dimensional characteristics $\overline{y} = AT\ x$. All samples are given covariance matrix,

$$q{=}\frac{1}{n}\sum_{q \in q}(q - m)(q - m)^T (14)$$

By obtaining the covariance matrix the features can be sort out.

The RMCA helps to optimize the feature selection process,

RMCA steps
➢ For the independent data group, estimate the mean Q dimensional vectors.
➢ Two methods, for example, between class and class to approximate the scatter matrices.
➢ To test the vectors and the associated scatter matrix authenticity values in a linear form.
➢ To select the proper vectors to form a scatter while decreasing their value and to select the proper vectors with the larger of their values (every column here represents a private vector)
➢ To transform the samples in a new subspace using the matrix of vector. The multiplication of the matrix can summarize this.

c. Segmentation
Then for the Segmentation, the CNN based multiscale phase level set segmentation method can be used**.** The level set's fundamental concept is to depict the hyper-surface curves and surfaces as a zero level range.

It provides more precise numerical and fast topological tests. The surface-smoothing method $\emptyset(x, y, z)$refers to the set-null-level method$\emptyset(x, y, z) = 0$. The whole surface may be viewed within and outside of the curve when using the curve as the boundary. To initialize this operation, the concept of input Distance (IDF) function on the surface is as follows equation (15).

$$\emptyset(x, y, z = 0) = D$$　　　　　(15)

Where,

　　　　Dis the shortest distance between the point x on the surface and curve.

_____

The general level set function is defined as follows in equation (16)

$$\emptyset_T + gD|\nabla\emptyset| = 0 \qquad\qquad (16)$$

Where,

F is the independent function depends on the information of images.

To improve the segmentation process, the independent internal term and the external independent term shall be considered. The gradient flow that reduces the cumulative power function is this growth.

$$E(\emptyset) = \min (E[e^T e]) = \min g(E | (t - \sigma)^T (t - \sigma)|) \qquad (17)$$

Where,

E is the controlling parameter.

σ is the Dirac delta function

g is the edge indicator function defined by

$$g_j = \sigma_j (1 - \sigma_j)(t_j - \sigma_j) \qquad\qquad (18)$$

I is an image, and g_j is the Gaussian kernel with standard deviation.

Algorithm (CNN based multiscale phase level set segmentation)

Input: Extract features

Output: Segment image

Initialize the multi-Network layers

Initialize train features T_{fea}

input size $i_{size} = 1$

No of hidden units $h_{units} = 100$

No of classes $N_{class} = 4$

maxEpochs $\epsilon_{size} = 100$

minibatch size $bat_{size} = 27$

Initialize label I_{label}

Train label = 80%

Tet label = 20%

* initialize the layers I_{layers}*

* initialize the options $I_{options}$*

Label = unique(label)

For ii = 1:lengh(Lab)

*   Class = find(label == Lab (ii))*

*   label I_{label} = categorical(I_{label})*

*   net = trainNetwork(T_{fea} , I_{label} , $I_{options}$)*

*   Traincut = length(class) - traincut*

*   Traindata = [traindata; trainfeatures; class(1: Traincut)end-5:end]*

*   Predict label = classify(net, traindata, bat_{size})*

End

End

For ii = 1:size(traindata,1)

* Traindata = [traindata; trainfeatures; class(1: Traincut)end-5:end]*

End

For ii = 1:size(trainfeatures,1)

*   Traindata = [trainfeatures;*

trainfeatures; class(1: Traincut)end-5:end]

End

d. 3D Reconstruction Modeling

Many images scanned by MRI colon, but the reconstruction requires considerable time and makes the algorithm complicated. Before starting up the process the images can be converted from JPEG to DICOM format. Then logical frustum model is applied to a segmented output. The step by step procedure of logical frustum model (LFM) is depicted below in figure 2.The three-dimensional (3D) displays provide the depth information which is unavailable in the 2D content.
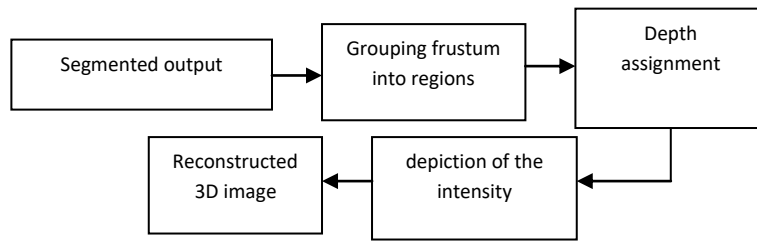
_____

Figure 2 3D image reconstruction

The paper describes the successful method of 2D to 3D conversion, based on edge data. Particularly the edge of an item is likely to be the edge of the map. The relative depth value of each area is assigned until the pixels are clustered together. The conceptual dissatisfaction paradigm that split the picture in multiple categories first. The depth of each segment is then calculated using an initial approximation of depth. Last but not least, the logical frustum method generates several views of the images. This converts the 2D image into a comfortable 3D image without artifacts improving image quality.

This implies each pixel in the same frustum has the same depth value. Here differentiate the image in the form of the frustum model. The value of each link between the frustum is calculated by considering the absolute difference of the mean of neighboring frustum.

Diff (n, d) =| Mean (n) − Mean (d) | 　　　　　(19)

where n and d denote two neighboring frustum blocks, respectively, and Mean (n) represents the mean. A smaller value implies that the two frustum blocks are more similar. The absolute difference in average of the nearby frustum blocks is calculated. And several grouped areas of frustration are created by removing the connections of stronger edges. The consistency between the frustum and connectivity unless many small groups are generated. This preserves the connectivity and also has a good spatial outcome. The efficient connection can effectively avoid the property of the image. Then the process can move on to the process of deep extraction. In the process of conversion, deep extraction is the key. Knowledge of 2D and 3D distance is the main difference. By collecting and combining these depth signals build a solid foundation for the refinement and development of 3D images. The required depth for each unit is then allocated with the assumed depth gradient after generation of the frustum block classes. The process consists of forming gradient plans, assigning the depth gradients and verifying the accuracy of the identified field.

$$Depth = \sum\nolimits_{Pixel\ (x,y)}[W_{frustum\ (1)}{}^{x-\frac{width}{2}}\Big/_{width} + W_{frustum\ (2)}{}^{x-\frac{height}{2}}\Big/_{height}]/\text{Pixel number(n)} \quad (20)$$

Greater depth indicates the proximity of the pixel. This formula shows that each block group has a depth function corresponding to the same degree as the block unit gravity centre. The meaning and $W_{frustum\ (1)}\ and\ W_{frustum\ (2)}$ sign can be balanced for the slope weight from left to right and from the top to bottom.This allows for the development of the depth chart. The graphical characteristics of the depth map are convenient since a bilateral cross-filter creates a seamless depth map with equivalent pixel values within the smooth region. The depth map can finally be created. A smooth depth map with equal pixel values within a smooth area retains sharp discontinuity at the object boundary with a comfortable visual consistency. The depth map is used then to create left / right or multi-visual images with 3D projection depth picture rendering. Finally, a pixel to the right or the left of the intermediate point can be identified for the 3D view. In other terms, the pixel position is adjusted according the depth quality. The 3D image can be reconstructed by using the below formula,

$$V_i = V_a + \left[\frac{t_V}{2} * \frac{f}{z}\right] (21)$$

The V i is the frustum view's horizontal coordinate, Z is the current pixel depth value, f is focal length and the t V eye width. The formula demonstrates the 3D image reconstruction of the intermediate pixel in horizontal direction from the left and right perspective.

The object area of any slice is then measured. A logical frustum model, in which the image can be reconstructed in a 3D way, shows the abnormality clearly. It is then used to measure the lymphoma volume for two in a row with Area Ai. An irregular object volume assessment is a key task, as the colon lymphoma is of no specific form. To overcome those restrictions, a bounding cube incorporates peculiar shapes such as a closed cube. The lymphoma volumes were determined using the three types of ellipse, sphere and cylinders. For the calculation of lymphoma volume the given formula is used.

$$V = \Sigma (\text{height}/4*(\text{area1} + \text{area 2} + (\text{area 1}* \text{area 2})1/2) \, P \qquad (22)$$

Height = thickness of the slice + splitting slice. The sum of areas of two consecutive slices gives the total volume of the lymphoma. Area 1 and area 2 display the regions of the two successive lymphoma slices.

5.RESULT AND DISCUSSION

The patient is divided by a related group of MRIs. More MRI slices were available for each of the three planes, Coronal, Axial and Sagittal. Any of these slices show that a tumour is present in a few parts. This tumour slices are selected manually and used after volume estimation for the tumour extraction sequence input. The entire process is performed in a matt laboratory setting. Colorectal MR pictures validated and compared to T2. The protocol suggested was applied. The data sets were collected from two separate hospitals Meenakshi Mission and Rajiv Gandhi Hospital of Madurai. The entire dataset was separated into training and test sets.
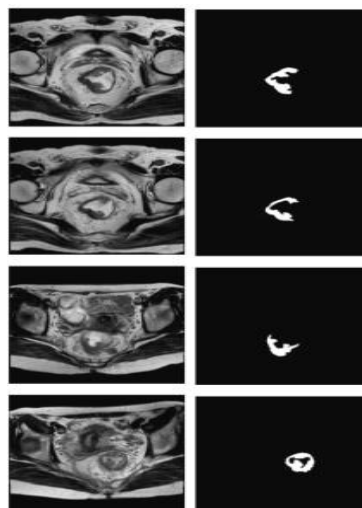

Figure 3 Colorectal tumor segmentation results

The findings for colorectal tumour segmentation obtained from the examinations indicate visually identical results in Figure 3. The first columns reflect the raw volume and volume of the MRI input, with the next related to the segmentation results produced by each technique in which each column shows the predictive probabilities with colorectal segmentation results. .
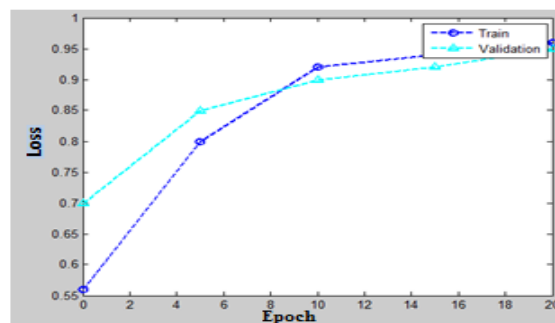

_____

Figure 4 Learning curves of the strategies under consideration are compared.

Figure 4 shows that no major over-fitting occurs in each procedure, since the performance loss decreases steadily and the formation loss decreases. It can be contrasted with [16] for the effectiveness of the proposed technique.
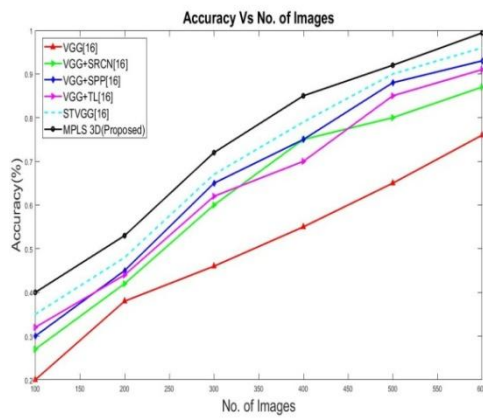

Figure 5 Accuracy prediction

From figure 5, it should be illustrated that the suggested methodology outperforms well when compared to other conventional methodology. CNN based Multiscale phase level set segmentation
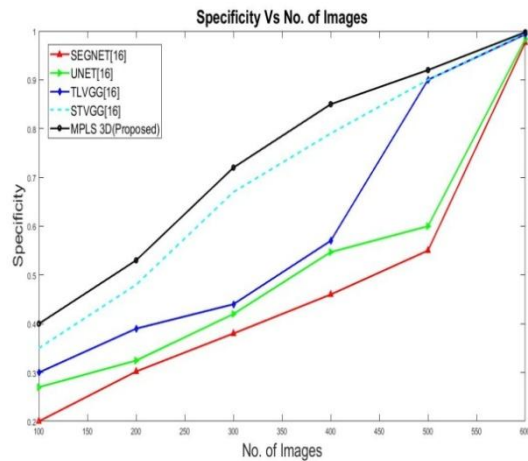

Figure 6 Prediction of specificity

The specificity of the individual negative measurements is often referred to as the real negative rate. From the above figure 6 it will reveals that when compared to other existing methodology the suggested CNN based Multiscale phase level set segmentation outperforms well by acquiring 99.9% specificity.
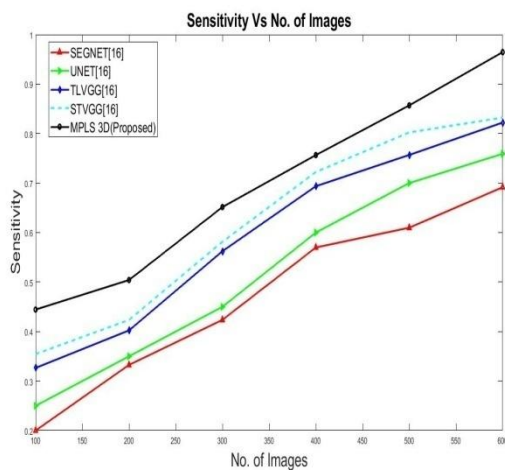

Figure 7 Sensitivity prediction

_____

Figure 7 shows that shows that the sensitivity comparison for proposed Multiscale phase level set segmentation method classifier. It is clear that the proposed method achieves Classification sensitivity of 98.9% and it accurately predicts colorectal cancer precisely.
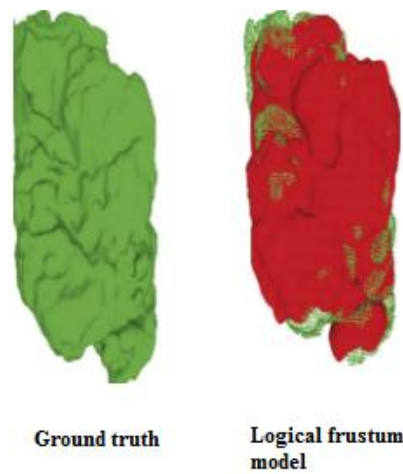

Figure 8 Logical frustum based 3D construction

As an input sequence for the 2D to 3D conversion, a segmented tumor result was presented using the algorithm of the Logical frustum model as shown in Figure 8.Tumor volume estimation

For the measurement of tumor size or length, the logical frustum model is used. For calculating the volume of the tumor, the formula is used.

$$\text{Volume} = \Sigma \ (\text{height}/3*(\text{Area1} + \text{Area2} + (\text{Area 1}* \text{Area 2})1/2)P \qquad (23)$$

Here in this process from the 3D converted image will sort out the tumor area. From that the tumor volume can be easily measured by using the above formula, Here from the 3D converted image,

Height=2mm,
A_1=12.56,
A_2=12.56The volume of the tumor =69.3 mg

Table 1Analysis of tumor volume

No	Slice	Total voxels	Area intensity mean	Area intensity SD	Pixel spacing (P in mm)	Thickness (H in mm)
1	1	5,782,400	1536	1781	0.35	2.0
2	8	4,970,766	917	1478	0.4	7.1
3	2	2,418,100	113	144	0.82	5.1
4	5	7,542,307	1240	1470	0.35	6.0

Table 1 indicates the volume determined by the sample tumor in terms of area values, as well as the approach suggested. By using the segmented results the volume measurement can be done.

6. CONCLUSION

The Colorectal Lymphoma is a life-threatening cause, triggering the elevated risk factor for humans. The Lymphoma identification method of the image processing process perfectly uses MR images for precise findings to detect the tumor as normal or abnormal. In this article, the segmentor used the prediction of an early-stage identification of a lymphoma. This chapter dealt with the performance analysis of proposed methodologies like a framework for CNN based multiscale phase level set segmentation of a Colorectal lymphoma in MRI

_____

images. Logical frustum model was used for the estimation of tumor volume and 3D visualization of MRI colorectal images. The results are evaluated, and the analysis shows that the proposed mechanism is better while comparing with other traditional techniques used so far. Thus, the result proves the effectiveness of using proposed techniques and is efficient than existing methods.Further extension of this research work can be done in the following ways:

This work can be extended to detect and diagnose liver fibrosis on the thermo gram images. Fuzzy rules can be built using fuzzy logic to improve the classification accuracy of colorectal diseases

7.REFERENCES

[1]   Y.-J. Huang *et al.*, "HL-FCN: Hybrid loss guided FCN for colorectal cancer segmentation," in *2018 IEEE 15th International Symposium on Biomedical Imaging (ISBI 2018)*, 2018, pp. 195-198: IEEE.

[2]   M. M. Abdelsamea, A. Pitiot, R. B. Grineviciute, J. Besusparis, A. Laurinavicius, and M. J. E. S. w. A. Ilyas, "A cascade-learning approach for automated segmentation of tumour epithelium in colorectal cancer," vol. 118, pp. 539-552, 2019.

[3]   Q. Li *et al.*, "Colorectal polyp segmentation using a fully convolutional neural network," in *2017 10th international congress on image and signal processing, biomedical engineering and informatics (CISP-BMEI)*, 2017, pp. 1-5: IEEE.

[4]   K. Wickstrøm, M. Kampffmeyer, and R. J. M. i. a. Jenssen, "Uncertainty and interpretability in convolutional neural networks for semantic segmentation of colorectal polyps," vol. 60, p. 101619, 2020.

[5]   D. Bychkov, R. Turkki, C. Haglund, N. Linder, and J. Lundin, "Deep learning for tissue microarray image-based outcome prediction in patients with colorectal cancer," in *Medical Imaging 2016: Digital Pathology*, 2016, vol. 9791, p. 979115: International Society for Optics and Photonics.

[6]   Q. Nguyen and S.-W. Lee, "Colorectal segmentation using multiple encoder-decoder network in colonoscopy images," in *2018 IEEE first international conference on artificial intelligence and knowledge engineering (AIKE)*, 2018, pp. 208-211: IEEE.

[7]   P. Wang and A. C. Chung, "DoubleU-Net: Colorectal Cancer Diagnosis and Gland Instance Segmentation with Text-Guided Feature Control," in *European Conference on Computer Vision*, 2020, pp. 338-354: Springer.

[8]   J. Kang and J. J. I. A. Gwak, "Ensemble of instance segmentation models for polyp segmentation in colonoscopy images," vol. 7, pp. 26440-26447, 2019.

[9]   X. Liu *et al.*, "Accurate colorectal tumor segmentation for CT scans based on the label assignment generative adversarial network," vol. 46, no. 8, pp. 3532-3542, 2019.

[10]   J. Panic *et al.*, "A Convolutional Neural Network based system for Colorectal cancer segmentation on MRI images," in *2020 42nd Annual International Conference of the IEEE Engineering in Medicine & Biology Society (EMBC)*, 2020, pp. 1675-1678: IEEE.

[11]   M. Marcan *et al.*, "Segmentation of hepatic vessels from MRI images for planning of electroporation-based treatments in the liver," vol. 48, no. 3, pp. 267-281, 2014.

[12]   A. Nelikanti, L. Narasimha Prasad, and M. Naresh Goud, *Colorectal Cancer MRI Image Segmentation Using Image Processing Techniques*. Citeseer, 2015.

[13]   L. Guachi, R. Guachi, F. Bini, and F. J. C. A. D. A. Marinozzi, "Automatic colorectal segmentation with convolutional neural network," vol. 16, no. 5, pp. 836-845, 2019.

[14]   J. Xu, X. Luo, G. Wang, H. Gilmore, and A. J. N. Madabhushi, "A deep convolutional neural network for segmenting and classifying epithelial and stromal regions in histopathological images," vol. 191, pp. 214-223, 2016.

[15]   M. Shaban *et al.*, "Context-aware convolutional neural network for grading of colorectal cancer histology images," vol. 39, no. 7, pp. 2395-2405, 2020.

[16]   Y. Yao, S. Gou, R. Tian, X. Zhang, and S. J. B. R. I. He, "Automated Classification and Segmentation in Colorectal Images Based on Self-Paced Transfer Network," vol. 2021, 2021.